Lens distortion correction with a calibration harp

Rafael Grompone von Gioi[1], Pascal Monasse[2], Jean-Michel Morel[1], Zhongwei Tang[1]

[1]Centre de Mathématiques et de Leurs Applications, Ecole Normale Supérieure de Cachan

[2]IMAGINE / CERTIS, Ecole des Ponts ParisTech

grompone@cmla.ens-cachan.fr, monasse@imagine.enpc.fr

morel@cmla.ens-cachan.fr, tang@cmla.ens-cachan.fr

Abstract – Plumb line lens distortion correction methods permit to avoid numerical compensation between the camera internal and external parameters in global calibration method. Once the distortion has been corrected by a plumb line method, the camera is ensured to transform, up to the distortion precision, 3D straight lines into 2D straight lines, and therefore becomes a pinhole camera. This paper introduces a plumb line method for correcting and evaluating camera lens distortion with high precision. The evaluation criterion is defined as the average standard deviation from straightness of a set of approximately equally spaced straight strings photographed uniformly in all directions by the camera, so that their image crosses the whole camera field. The method uses an easily built "calibration harp," namely a frame on which strings have been tightly stretched to ensure a very high physical straightness. Real experiments show that the correction precision also depends on the quality of strings. With good quality fishing strings, our method produces high precision corrections (about 0.02 pixel), approximating the distortion with a moderate number of degrees of freedom given by a polynomial model of order eleven.

1 Introduction

This paper presents a method to correct camera lens distortion with high precision. By high precision, we mean deviations from straightness of less, or far less than 0.1 pixel for a straight line crossing the whole camera field. Such a precision is hardly appreciable for a human observer. However, there is no limit to the desired precision when the camera is used for 3D reconstruction or photogrammetry tasks. Traditionally, lens distortion and the other camera parameters are estimated simultaneously as camera internal and external parameters [1, 2, 3, 4, 5]. In these global calibration methods all parameters are estimated by minimizing the error between the camera and its numerical model on feature points identified in several views, all in a single non-linear optimization. The result will be precise if (and only if) the model captures the correct physical properties of cameras and if the minimization algorithm finds a global minimum. Unfortunately, global camera calibration suffers a common drawback: errors in the external and internal camera parameter can be compensated by opposite errors in the distortion model. Thus the residual error can be apparently small, while the distortion model is not precisely estimated [5, 6]. For example, the Lavest et al. method [4] measures the non-flatness of a pattern and yields a remarkably small re-projection error of about 0.02 pixels, while the straightness of corrected lines has a 0.2 pixel RMSE. Fortunately the error compensation in global calibration can be avoided by proceeding to distortion correction before camera calibration. Recent distortion correction methods use the correspondences between two or several images, without knowledge of any camera information. The tool of slackened epipolar constraints, which incorporate a simple low-order distortion model into the epipolar geometry, is used to estimate the distortion [7, 8, 9, 10, 11, 6, 12].

Non-parametric methods which establish a direct diffeomorphism between a flat pattern and a frontal photograph of it [13, 14] should be ideal for high precision distortion correction. Indeed, they do not depend on the *a priori* choice of a distortion model with a fixed number of parameters. Yet to achieve a high precision, they depend on the design of a very flat non deformable plate with highly accurate patterns printed on it.[1] This replaces a technological challenge by another, which is not simpler. Plumb-line methods [15] should therefore be an alternative because, as we shall see, it is easier to create very straight lines, even though the precision of distortion correction also depends on the quality of lines, as we will see in the experiments. For plumb-line methods, a distortion model is still necessary to precisely remove the distortion, and most existing models can be used. Nevertheless, some of them are too complicated [15], while some are not general enough to capture the distortion [16]. For most distortion models, the distortion center is a sensitive parameter when a realistic distortion is treated. The barely polynomial approximation proposed in [17] is therefore a good choice, being a translation invariant and linear approximation of any vector field. This model-free formulation can

[1]A 10 μm flatness could be needed to achieve a precision of 0.01 pixels.

approximate complex radial and non-radial distortions as well, provided the polynomial degree is high enough. According to the criteria of *self-consistency* and *universality*[2] developed in [17] to compare many camera distortion models, the polynomial models are the most flexible and accurate.

The proposed method is introduced in section 2, followed by real experiments in section 3, along with a comparison to a non-parametric method. Section 4 concludes the paper.

2 The harp calibration method

In one sentence, the proposed method combines the advantage of plumb-line methods with the universality of the polynomial approximation. The plumb-line method consists in correcting the distorted points which are supposed to be on a straight line, by minimizing the average squared distance from the corrected points to their corresponding regression lines.

The polynomial model has the form

$$\begin{aligned} x_u &= b_0 x_d^p + b_1 x_d^{p-1} y_d + b_2 x_d^{p-2} y_d^2 + \cdots + b_p y_d^p \\ &\quad + b_{p+1} x_d^{p-1} + b_{p+2} x_d^{p-2} y_d + \cdots + b_{2p} y_d^{p-1} \\ &\quad + \cdots + b_{\frac{(p+1)(p+2)}{2}-3} x_d + b_{\frac{(p+1)(p+2)}{2}-2} y_d \\ &\quad + b_{\frac{(p+1)(p+2)}{2}-1} \\ y_u &= c_0 x_d^q + c_1 x_d^{q-1} y_d + c_2 x_d^{q-2} y_d^2 + \cdots + c_q y_d^q \\ &\quad + c_{q+1} x_d^{q-1} + c_{q+2} x_d^{q-2} y_d + \cdots + c_{2q} y_d^{q-1} \\ &\quad + \cdots + c_{\frac{(q+1)(q+2)}{2}-3} x_d + c_{\frac{(q+1)(q+2)}{2}-2} y_d \\ &\quad + c_{\frac{(q+1)(q+2)}{2}-1} \end{aligned} \quad (1)$$

with (x_u, y_u) undistorted point and (x_d, y_d) distorted point. The polynomial approximation being translation invariant, the origin is arbitrarily fixed at the image center. The order for the x and y components is respectively p and q. The number of parameters for x and y is respectively $\frac{(p+1)(p+2)}{2}$ and $\frac{(q+1)(q+2)}{2}$. The model is called bicubic model when $p = q = 3$.

In the following, we show how to integrate the polynomial model into the plumb-line method. Given a set of corrected points $(x_{u_i}, y_{u_i})_{i=1,\cdots,N}$ which are supposed to be on a line, the first step is to compute the linear regression line

$$\alpha x_{u_i} + \beta y_{u_i} - \gamma = 0 \quad (2)$$

where α, β and γ can be parameterized by the coefficients of the polynomial model. The sum of squared distances from the points to this regression line can be computed as $\sum_{i=1}^{N} (\alpha x_{u_i} + \beta y_{u_i} - \gamma)^2$. By considering G groups of lines, the total sum of squared distance is

$$S = \sum_{g=1}^{G} \sum_{l=1}^{L_g} \sum_{i=1}^{N_{gl}} (\alpha_g x_{u_{gli}} + \beta_g y_{u_{gli}} - \gamma_{gl})^2 \quad (3)$$

with L_g the number of lines in group g, and N_{gl} the number of points of line l in group g. Given the total number of points $N = \sum_{g=1}^{G} \sum_{l=1}^{L_g} N_{gl}$, the root mean squared distance (RMS error) is defined by

$$d = \sqrt{\frac{S}{N}}. \quad (4)$$

For a sake of succinctness, the following discussion will assume a bicubic model with $p = q = 3$. Combining Eq. (1) and Eq. (3), the energy S becomes

$$\begin{aligned} S &= \sum_{g=1}^{G} \sum_{l=1}^{L_g} \sum_{i=1}^{N_{gl}} \Big(\alpha_g \big(b_0 x_{d_{gli}}^3 + \cdots + b_9 \big) \\ &\quad + \beta_g \big(c_0 x_{d_{gli}}^3 + \cdots + c_9 \big) - \gamma_{gl} \Big)^2. \end{aligned} \quad (5)$$

The minimization of the energy in Eq. (5) is a non-linear problem with respect to the parameters $b_0, \ldots, b_9, c_0, \ldots, c_9$. The problem becomes linear when the orientation parameters α_g, β_g are known. In practice, however, the orientation of lines is unknown.

To obtain a unique non-trivial solution, we always set $b_7 = c_8 = 1$, $b_9 = c_9 = 0$ (when $p = q = 3$), which in fact fixes a scale and a translation to the solution. The minimized S can be changed by the introduced scale. But this change is consistent if the distortion center and b_9, c_9, b_7, c_8 are fixed. The minimization is performed by first doing an iterative Levenberg-Marquardt (LM) algorithm which estimates the parameters of polynomials of increasing order. The algorithm starts estimating the parameters of a 3-order polynomial; the result is used to initialize the 4-order polynomial, and the process continues until 11-order. After this first step, the linear estimation is performed iteratively to refine the precision. The line orientations are first initialized by the orientation of the regression lines obtained by the LM method, and then with the values of the previous linear step. The iteration is repeated until the results stabilize or the required precision is reached. An example of error evolution in the minimization process is shown in Table 1.

3 Experiments

In this section, we describe real experiments with a strong distortion comparing the performance of the proposed method with a harp made up of sewing strings and a harp made up of fishing strings.

The experiments were made with a Canon EOS 30D reflex camera with EFS $18-55$mm lens. The minimal

[2] Self-consistency is evaluated by the residual error when distortion generated with a certain model is corrected (using the model in reverse way) by the best parameters for the same model. Analogously, universality is measured by the residual error when a model is used to correct distortions generated by a family of other models. A model is self-consistent and universal if it can approximate any other model and the inverse of any other model, including itself, with the desired precision. As shown in [17], polynomials of order 11 are 0.01 pixels self-consistent and universal.

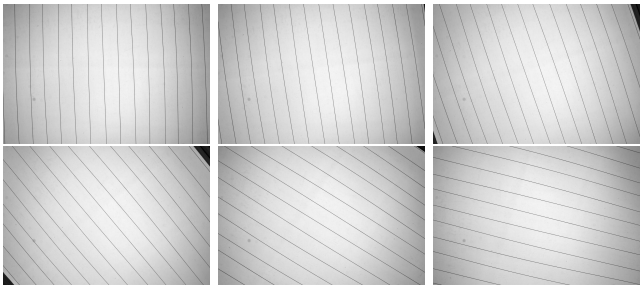

FIG. 1: Six of the 18 photos of the fishing string calibration harp with different orientation. The photos of the sewing string calibration harp look similar. See the detail of the string in Fig 2.

FIG. 2: A detail of the string. Left: sewing string. Right: fishing string.

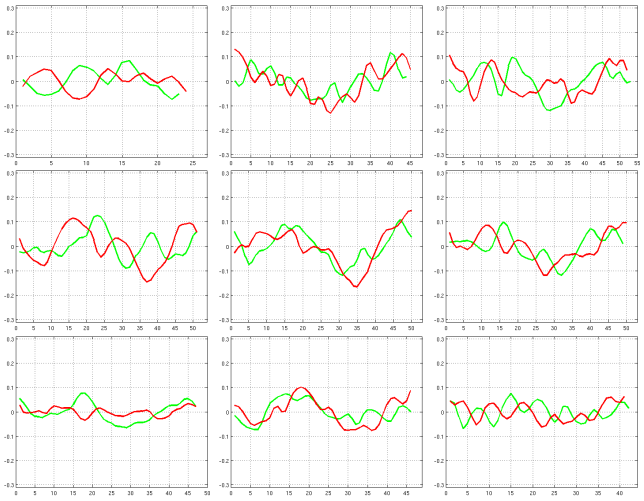

FIG. 3: Correction performance of the proposed method with a sewing string harp. An independent image not used in the polynomial model estimation was used here to measure the correction precision. The curve shows the distance from the edge point of the corrected lines to their corresponding regression line. Note that each figure contains two curves because there are two lines for one string. The x-axis is the index of edge points. The range of y-axis is from -0.3 pixels to 0.3 pixels.

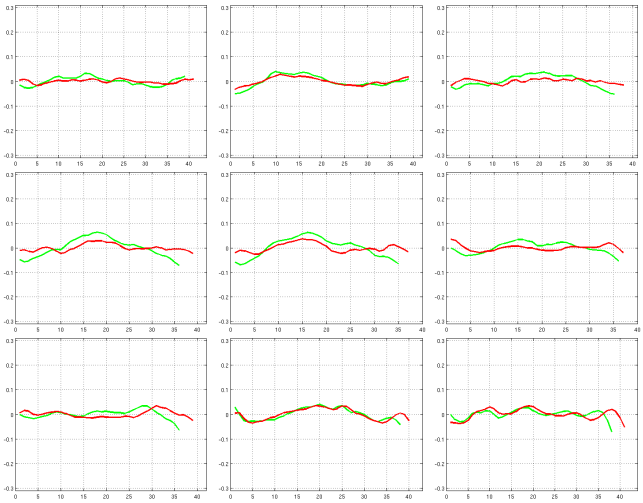

FIG. 4: Correction performance of the proposed method with a fishing string harp. See the caption of Fig. 3 for details.

focal length (18mm) was chosen to produce a fairly large distortion. The RAW images were demosaicked by summing up the four pixels of each 2×2 Bayer cell, obtaining a half-size image. Two calibration harps were built: one was made up of sewing strings and the other fishing strings (see the detail of the strings in Fig. 2). Both strings were stretched tightly to ensure a very high physical straightness. A high distortion is visible near the border of the image (see the images in Fig. 1 for example). The same experiment was repeated with two harps: 18 photographs of the calibration harp with different orientations were used in the calibration by the 11-degree polynomial model (a 5-order polynomial model can be used to accelerate the minimization process according to Table 1). An independent distorted image is used for verification. The lines were detected as follows: sub-pixel precise edge points were obtained by Devernay's algorithm [18] and then grouped when belonging to the same line segments detected by the LSD algorithm [19].

The correction result of the sewing string harp and the fishing string harp is recapitulated in Fig. 3 and 4 respectively. Note that in both figures, the y-axis has the same range, from -0.3 pixels to 0.3 pixels. As shown in both figures, the distortion correction is so accurate that no visible global tendency is visible in the corrected curves. The result of the sewing string harp is more oscillating than that of the fishing string harp. This is in fact due to the quality of strings. Indeed, the observed oscillation inherits the high frequency of the distorted lines, while lens distortion alters only the low frequency of the distorted lines. In Fig. 2, the sewing string has a twisted structure while the fishing string is more smooth. The oscillation in Fig. 3 is due to a variation of the thickness related to the twisted structure of the sewing string. The result in Fig. 4 shows smaller oscillation thanks to the smoothness

of the fishing string.

minimization		RMSE (in pixels)	
		sewing string harp	fishing string harp
LM order	3	0.42	0.46
	4	0.42	0.45
	5	0.08	0.06
	6	0.08	0.05
	7	0.07	0.04
	8	0.07	0.04
	9	0.06	0.04
	10	0.06	0.04
	11	0.06	0.04
linear step		0.04	0.03

TAB. 1: The average RMSE evolution in the minimization process. The minimization is composed of an incremental LM algorithm from order 3 to 11, followed by a linear minimization.

4 Conclusion

By combining the advantages of a model-free polynomial approximation and of a real plumb line pattern, the proposed lens distortion correction achieves precisions of about 0.02 pixels. The "calibration harp" construction only requires the acquisition of a string with decent quality. It is far simpler than realizing a flat plate with highly accurate patterns engraved on it. (The calibration of such patterns is not easier than lens calibration itself!) The high number of degrees of freedom in the unstructured model explains why we can call the method model-free. The only assumption on the lens distortion is its smoothness, implying that a polynomial with high enough order approximates it. In our experiments, the approximation error stabilizes for polynomials of degree 7 to 11. It might be objected that the high number of parameters in the polynomial interpolation (156 for an 11-order polynomial) could cause some bias in the result. Yet, the number of control points is far higher: There were about 10 strings for each orientation, some 30 control points on each string side, and some 18 orientations. Thus the number of control points is about 10000 and therefore 60 times more than the number of polynomial coefficients. A visual examination of the two sides of the strings confirms that no artificial simultaneous bias has been introduced by the polynomial distortion correction. Another interesting observation is that the correction only changes the low frequency of distorted lines. The high frequency, which is related to the quality of strings, will be inherited by the corrected lines. This motivated us to use the fishing string to fabricate the calibration harp, which produces a correction result more precise than the sewing string harp. Future work will concentrate on the precision of external camera calibration, and eventually on the 3D precision after having removed the lens distortion by the present method.

References

[1] C. C Slama, *Manual of Photogrammetry, 4th edition*, Falls Church, American Society of Photogrammetry, Virginia, 1980.

[2] Roger Y. Tsai, "A versatile camera calibration technique for high-accuracy 3D machine vision metrology using off-the-shelf tv cameras and lenses," *IEEE Journal of Robotics and Automation*, vol. Vol. RA-3, 1987.

[3] Z. Zhang, "A flexible new technique for camera calibration," *ICCV*, pp. 663–673, Sept. 1999.

[4] J. Lavest, M. Viala, and M. Dhome, "Do we really need accurate calibration pattern to achieve a reliable camera calibration?," *ECCV*, vol. 1, pp. 158–174, 1998.

[5] J. Weng, P. Cohen, and M. Herniou, "Camera calibration with distortion models and accuracy evaluation," *TPAMI*, vol. 14(10), pp. 965–980, 1992.

[6] H. Li and R. Hartley, "A non-iterative method for correcting lens distortion from nine point correspondences," *OmniVis*, 2005.

[7] Gideon P. Stein, "Lens distortion calibration using point correspondences," *CVPR*, p. 602608, 1997.

[8] Z. Zhang, "On the epipolar geometry between two images with lens distortion," *ICPR*, pp. 407–411, 1996.

[9] T. Pajdla and B. Micusik, "Estimation of omnidirectional camera model from epipolar geometry," *CVPR*, pp. 485–490, 2003.

[10] A. W. Fitzgibbon, "Simultaneous linear estimation of multiple view geometry and lens distortion," *CVPR*, vol. 1, pp. 125–132, 2001.

[11] J.P. Barreto and K. Daniilidis, "Fundamental matrix for cameras with radial distortion," *ICCV*, vol. 1, pp. 625–632, 2005.

[12] D. Claus and A.W. Fitzgibbon, "A rational function lens distortion model for general cameras," *CVPR*, vol. 1, pp. 213–219, 2005.

[13] R. Grompone von Gioi, P. Monasse, J.-M. Morel, and Z. Tang, "Towards high-precision lens distortion correction," *ICIP*, pp. 4237–4240, 2010.

[14] D. Stevenson and M.M. Fleck, "Nonparametric correction of distortion," Tech. Rep., omp. Sci., U. of Iowa, 1995.

[15] D.C. Brown, "Close-range camera calibration," *Photogrammetric Engieering*, vol. 37, pp. 855–866, 1971.

[16] F. Devernay and O. Faugeras, "Straight lines have to be straight," *Mach. Vision Appli.*, vol. 13, pp. 14–24, 2001.

[17] R. Grompone von Gioi, P. Monasse, J.-M. Morel, and Z. Tang, "Self-consistency and universality of camera lens distortion models," *CMLA Preprint, ENS-Cachan*, 2010.

[18] F. Devernay, "A non-maxima suppression method for edge detection with sub-pixel accuracy," Tech. Rep. 2724, INRIA rapport de recherche, 1995.

[19] R. Grompone von Gioi, J. Jakubowicz, J.-M. Morel, and G. Randall "LSD: A fast line segment detector with a false detection control," *IEEE TPAMI*, vol. 32, no. 4, pp. 722-732, 2010.